

Bound pulse trains in arrays of coupled spatially extended dynamical systems

D. Puzyrev¹, A. G. Vladimirov^{2,3}, A. Pimenov², S. V. Gurevich^{4,5}, S. Yanchuk¹

¹*Institute of Mathematics, Technische Universität Berlin,
Strasse des 17. Juni 136, D-10623 Berlin, Germany*

²*Weierstrass Institute for Applied Analysis and Stochastics, Mohrenstrasse 39, D-10117 Berlin, Germany*

³*Lobachevsky State University of Nizhni Novgorod,
pr. Gagarina 23, Nizhni Novgorod, 603950, Russia*

⁴*Institute for Theoretical Physics, University of Münster,
Wilhelm-Klemm-Str. 9, D-48149 Münster, Germany*

⁵*Center for Nonlinear Science (CeNoS), University of Münster, Corrensstr. 2, D-48149 Münster, Germany*

We study the dynamics of an array of nearest-neighbor coupled spatially distributed systems each generating a periodic sequence of short pulses. We demonstrate that unlike a solitary system generating a train of equidistant pulses, an array of such systems can produce a sequence of clusters of closely packed pulses, with the distance between individual pulses depending on the coupling phase. This regime associated with the formation of locally coupled pulse trains bounded due to a balance of attraction and repulsion between them is different from the pulse bound states reported earlier in different laser, plasma, chemical, and biological systems. We propose a simplified analytical description of the observed phenomenon, which is in a good agreement with the results of direct numerical simulations of a model system describing an array of coupled mode-locked lasers.

Nonlinear temporal pulses and spatial dissipative localized structures appear in various optical, plasma, hydrodynamic, chemical, and biological systems [1–13]. Being well-separated from each other these structures can interact locally via exponentially decaying tails and, as a result of this interaction, they can form bound states, known also as “dissipative soliton molecules” [14], characterized by fixed distances and phase differences between individual structures. Such bound states can emerge due to the oscillatory character of the interaction force which is related to the presence of oscillating tails. Another scenario occurs in the case of monotonic repulsive interaction when either the pulse tails decay monotonically, or a strong nonlocal repulsive interaction between the pulses is present. In this case the pulses tend to distribute equidistantly in time or space leading to periodic pulse trains [15–18] which, in contrast to closely packed bound states, exhibit large distances between the consequent pulses.

In this Letter we show that even in the case when the pulses in an individual system exhibit strong repulsion, the formation of bound pulse trains can be achieved by arranging several systems in an array with nearest-neighbor coupling. As a result, the pulses interact not only within one system, but also with those in the neighboring ones leading to a different balance of attraction and repulsion. More specifically, we demonstrate that this array can produce a periodic train of clusters consisting of two or more closely packed pulses with the possibility to change the interval between the pulses via the variation of coupling phase parameter. We show that the observed pulse train states coexist with the regimes which are amplitude synchronized and possess fixed phase shifts between the pulses emitted by neighboring array elements. In contrast to the pulse bound state regimes predicted and observed experimentally previously [14, 19–32], this regime cannot exist in a solitary pulse-generating

system. We illustrate this general result by considering a particular example of an array of mode-locked lasers coupled via evanescent fields in a ring geometry. Such lasers are widely used for generation of short optical pulses with high repetition rates and optical frequency combs suitable for numerous applications. Combining many lasers into an array one can achieve much larger output power and substantially improve the characteristics of the output beam by synchronizing the frequencies of the individual lasers [33–40]. Furthermore, it was recently demonstrated experimentally and verified theoretically that, in contrast to broad area lasers suffering from transverse instabilities leading to poor output beam quality, phase synchronization of individual elements of a multistripe semiconductor laser arrays can be used to generate high power beams with low far-field divergence [41, 42].

The correspondence between spatially extended and time-delay systems was established in series of publications [43–46]. In particular, it was shown that delay differential equations (DDEs) can be reduced to the well known Ginzburg-Landau amplitude equation in a vicinity of a bifurcation point. On the other hand, many problems expressed in terms of partial differential equations can be reformulated in terms of DDEs [47]. Therefore, for our analysis it is convenient to assume that each individual array element generating a periodic pulse train is described by a set of DDEs. Then the dynamics of an array of N such elements can be described by the set of symmetrically coupled systems of nonlinear DDEs

$$\frac{d\vec{u}_j}{dt} = \vec{F}[\vec{u}_j(t), \vec{u}_j(t - \tau)] + C(\vec{u}_{j-1} + \vec{u}_{j+1}). \quad (1)$$

Here \vec{u}_j , $j = 1, \dots, N$ is the state variable describing the j -th system and C is the coupling matrix. We assume that in the absence of coupling, $C = 0$, system generates periodic pulses with the period close to the delay time τ . In our simulations we use a partic-

ular model describing a mode-locked laser [47]. There, $\vec{u} = (A(t), G(t), Q(t))^T$, where A denotes the complex electric field amplitude, whereas G and Q are saturable gain and loss, respectively. The components of the right hand side vector function \vec{F} are defined by $F_1 = -\gamma A + \gamma\sqrt{\kappa}RA(t-\tau)$, $F_2 = G_0 - \gamma_g G - e^{-Q}(e^G - 1)|A(t-\tau)|^2$, and $F_3 = Q_0 - \gamma_q Q - s(1 - e^{-Q})|A(t-\tau)|^2$, with $R := \exp[(1 - i\alpha_g)G - (1 - i\alpha_q)Q]/2 - i\vartheta$. Here, the parameter γ represents the spectral filtering bandwidth, κ is the attenuation factor describing linear non-resonant intensity losses per cavity round trip, G_0 is the pump parameter, which is proportional to the injection current in the gain region, Q_0 is the unsaturated absorption parameter, γ_g and γ_q are the carrier relaxation rates in the amplifying and absorbing sections, and s is the ratio of the saturation intensities in these two sections. Though all the parameter values can vary among different lasers, we assume that this variation is sufficiently small and consider equal parameters. In what follows we limit our analysis to the physically meaningful situation when the lasers are coupled via evanescent fields and, hence, the coupling matrix C has only a single nonzero element $C_{11} = \eta e^{i\varphi}$, where η is the coupling strength and φ is the coupling phase.

In the absence of coupling, $\eta = 0$, for the chosen parameter values each laser operates in a stable fundamental passive mode-locking regime with a single sharp pulse per cavity round trip time [47]. This regime corresponds to modulated waves (relative periodic orbits) with $A_j(t) = U(t - \theta_j)e^{i\omega t + i\nu_j}$, $G_j = G(t - \theta_j)$, and $Q_j = Q(t - \theta_j)$, where $U(t)$, $G(t)$, and $Q(t)$ are periodic in time with the period T close to the delay τ , and arbitrary phase shifts θ_j and ν_j .

For small coupling η , the phase shifts θ_j and ν_j start evolving slowly in time due to the interaction between the lasers and, as a result, a synchronized state can be achieved. In particular, due to the index shift symmetry of the system, solutions are observed, that are synchronized in the amplitude $|A_j| = |A|$ and with the constant phase shift between the adjacent lasers $\nu_{j+1} - \nu_j = 2\pi l/N$, $l = 0, \dots, N-1$ [39, 40, 48–50]. The simplest types of the synchronized regimes are complete in-phase synchronization ($l = 0$) and anti-phase synchronization ($l = N/2$) for even number of lasers N . Note, that there is also a potentially interesting "non-invasive" case $l = N/4$, for which the coupling vanishes $A_{j-1} + A_{j+1} = 0$. For odd values of N , however, the anti-phase and non-invasive synchronization regimes do not exist.

Further we consider the minimal cases of $N = 2$ and $N = 4$ lasers, where $N = 4$ is the smallest number that allows in-phase, anti-phase, and non-invasive synchronized solutions. Figure 1(a) demonstrates the stability regions for the in-phase and anti-phase synchronized mode-locked solutions of the system of four lasers using the master stability function approach [51] in the (φ, η) plane of coupling parameters. The form of coupling implies that the stability region of the anti-phase

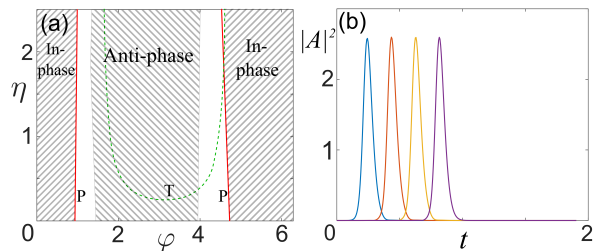


Figure 1. (a) Bifurcation diagram in coordinates (φ, η) for the synchronized solutions in the ring array of four lasers. Left- and right-inclined hatching indicates the stability regions for the in-phase ($l = 0$) and anti-phase ($l = 2$) synchronized solutions. Green line corresponds to a torus bifurcation (T) and red lines to pitchfork bifurcations (P) of the in-phase synchronized solution. (b) Laser intensities for the pulse train bound-state regime in a ring of four lasers calculated for $\eta=0.5$ and $\varphi = 3.0$. Different colors correspond to different lasers. Other parameters: $\gamma = 33.3$, $\kappa = 0.1$, $\alpha_g = 2.0$, $\alpha_q = 3.0$, $\vartheta = 0$, $G_0 = 2.0$, $Q_0 = 4.0$, $\gamma_g = 0.0133$, $\gamma_q = 1$, $s = 25$, and $\tau = 1.875$ (similarly to [47]).

synchronized solution coincides with that of the in-phase synchronized solution shifted by π with respect to the coupling phase angle φ . Furthermore, the P and T lines in Fig. 1 (a) show bifurcation thresholds of the in-phase synchronized regime ($l = 0$). In particular, the green line (T) indicates a torus bifurcation threshold whereas the two red lines correspond to pitchfork bifurcations.

The torus bifurcation leads to a slight change of the pulse shape from one pulse period to another, while synchronization and period of pulsing remains the same. Instead, the pitchfork bifurcations of the synchronized solution leads to the appearance of a new *bound pulse train regime*. In this regime, lasers pulse sequentially on the ring one after another, as shown in Fig. 1(b). Here, each laser stays close to its fundamental mode-locked regime with period τ_0 close to the delay time τ . The pulse train bound-state regime can be better visualized using the so-called pseudo-spatial coordinates plane (T, σ) [46], where $\sigma = t \bmod \tau_0$ is the original fast time and $T = t/\tau_0$ is the slow time (number or round trips, $\tau_0 = \tau + 0.03$), see Fig. 2(a). We observe that pulses which were initially distributed on the interval $\sigma \in [0, \tau_0]$ start to interact and finally form a bound cluster. The distance between the pulses in this cluster can be controlled by changing the coupling phase φ . Similar bound pulse train for the case of two coupled lasers is shown in Fig. 2(b). In what follows, we investigate the origin of this bound state solution by applying the multiscale method [52, 53] to the two-laser system in order to find the reduced system of equations governing the slow dynamics of the time separation between the pulses and their phase differences.

In order to use the multiscale method, we consider the limit of small coupling, $\eta = \varepsilon\mu$ with a small parameter ε , and search for the solution of system (1) in

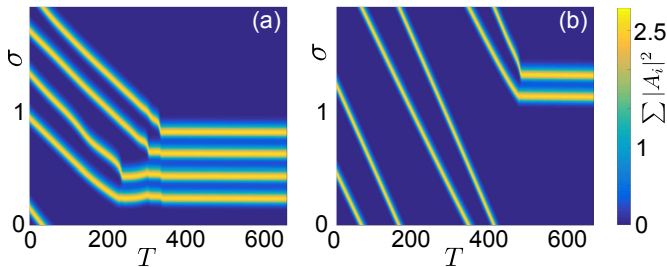


Figure 2. (a) Space-time diagram of the pulse train bound-state regime for four lasers in coordinates (T, σ) , where $\sigma = t \bmod \tau_0$ is the original fast time and $T = t/\tau_0$ the slow time ($\tau_0 = 1.9054$). Brighter colors indicate higher values of the sum of the laser intensities $\sum_{i=1}^4 |A_i|^2$. (b) Space-time diagram for pulse train bound state regime for two lasers ($\tau_0 = 1.9043$). Coupling parameters are: $\eta=0.5$, $\varphi = 3.0$.

the form $A_j(t_0, t_1) = e^{i\phi_j(t_1)} \mathcal{A}[t_0 + \theta_j(t_1)] + \varepsilon A_j^1(t_0, t_1)$, $G_j = \mathcal{G}[t_0 + \theta_j(t_1)] + \varepsilon G_j^1(t_0, t_1)$, $Q_j = \mathcal{Q}[t_0 + \theta_j(t_1)] + \varepsilon Q_j^1(t_0, t_1)$. Here \mathcal{A} , \mathcal{G} , and \mathcal{Q} is a τ_0 -periodic solution of the unperturbed system (mode-locked regime in an uncoupled laser), A_j^1 , G_j^1 , Q_j^1 describe first order corrections due to the coupling between the lasers, $t_0 = t$ and $t_1 = \varepsilon t$ are fast and slow times, respectively.

In the following, we explain how the reduced system (7) for the time separation $\Theta = \theta_2 - \theta_1$ between the pulses and the phase difference $\Phi = \phi_2 - \phi_1$ between pulses peaks can be obtained. For this purpose, the ansatz above is substituted into (1) and the resulting system is expanded in orders of ε (see [52, 53] for more details on this method). In the order $\mathcal{O}(\varepsilon)$, the following linear system of DDEs for the vector of perturbations $S_j = (\text{Re } A_j^1, \text{Im } A_j^1, G_j^1, Q_j^1)^T$ is obtained

$$\begin{aligned} -\dot{S}_j + a_1(t) S_j(t) + a_2(t) S_j(t - \tau) = \\ a_3 \dot{\theta}_j + a_4 \dot{\phi}_j + \mathcal{R}((-1)^j \Theta, (-1)^j \Phi), \end{aligned} \quad (2)$$

$j = 1, 2$, with linear operators $a_{1,2}$ and vector functions $a_{3,4}$ depending only on the unperturbed pulse solution. Expressions for $a_{1,2,3,4}$ and \mathcal{R} are given in the Supplemental material.

The solvability condition (for bounded solutions) of the linear non-homogeneous system (2) requires that its right hand side is orthogonal to the neutral (or Goldstone) modes of the adjoint homogenous system [54]. In the case of small coupling coefficient, $\eta \ll 1$, these modes can be approximated by ψ_j^\dagger and ξ_j^\dagger with $j = 1, 2$, that are related to the phase shift and the time-shift invariance of the model equations. These modes can be found numerically (see, e.g. [52, 53]). The orthogonality of the right hand side of (2) to $\psi_{1,2}^\dagger$ with respect to the inner product $\int_0^T (a_3 \dot{\theta}_j + a_4 \dot{\phi}_j + \mathcal{R}((-1)^j \Theta, (-1)^j \Phi)) \psi_j^\dagger(t) dt = 0$

leads to the system of two ordinary differential equations

$$p_\psi \dot{\theta}_1 + q_\psi \dot{\phi}_1 = \mu R_\psi(\Theta, \Phi), \quad (3)$$

$$p_\psi \dot{\theta}_2 + q_\psi \dot{\phi}_2 = \mu R_\psi(-\Theta, -\Phi), \quad (4)$$

where coefficients p_ψ , q_ψ , and R_ψ are given by the corresponding scalar products cf. the Supplemental material. Subtracting equations (3) and (4) from one another, one obtains the equation for the phase difference Φ and time separation of the pulses Θ :

$$p_\psi \dot{\Theta} + q_\psi \dot{\Phi} = \mu (R_\psi(-\Theta, -\Phi) - R_\psi(\Theta, \Phi)). \quad (5)$$

In the same way, the orthogonality conditions to the modes $\xi_{1,2}^\dagger$ lead to the equation

$$p_\xi \dot{\Theta} + q_\xi \dot{\Phi} = \mu (R_\xi(-\Theta, -\Phi) - R_\xi(\Theta, \Phi)). \quad (6)$$

Solving now (5) and (6) for $\dot{\Theta}$ and $\dot{\Phi}$, we obtain the reduced system of two ordinary differential equations for the slow time evolution of Θ and Φ :

$$\begin{aligned} \dot{\Theta} &= \eta \cos(\Phi + \Delta_\Theta(\Theta)) f_\Theta(\Theta), \\ \dot{\Phi} &= \eta \sin(\Phi + \Delta_\Phi(\Theta)) f_\Phi(\Theta), \end{aligned} \quad (7)$$

where $f_{\Theta, \Phi}(\Theta) \geq 0$. The specific shape of the right hand side of (7) is due to the fact that the function $R_\psi(\Theta, \Phi)$ contains only first Fourier harmonic in Φ . As a result, the dependence on Φ is a linear combination of $\sin(\Phi)$ and $\cos(\Phi)$ that can be represented as (7). More details are given in the Supplemental material.

The bound pulse train states correspond to the fixed points of (7). These points lying on the intersection of nullclines of (7) are defined by the condition $\cos(\Phi + \Delta_\Theta(\Theta)) = \sin(\Phi + \Delta_\Phi(\Theta)) = 0$, which implies that one of the two conditions should be satisfied, $\Delta_\Theta(\Theta) = \Delta_\Phi(\Theta)$, or $\Delta_\Theta(\Theta) = \Delta_\Phi(\Theta) + \pi$. The first condition corresponds to the saddles of the system (7), while the second equation corresponds either to nodes or to foci. Figure 4(a) shows intersecting nullclines of (7) in the (Θ, Φ) phase plane. Here, blue filled (unfilled) circles depict stable (unstable) nodes, red filled (unfilled) circles correspond to stable (unstable) foci, and blue squares – to saddles. All of these equilibria correspond to pulse bound states in system (1) with the same stability properties. Note that a particular case $\Theta = 0$ corresponds to the synchronized pulses with the zero time separation, when the system (7) transforms into a single equation $\dot{\Phi} = \mu C_\Phi \sin \Phi$, which admits either in-phase $\Phi = 0$ or anti-phase synchronization $\Phi = \pi$ as it was mentioned above.

Noteworthy, the reduced system (7) resembles the equations governing the slow dynamics of the distance and phase difference between two interacting dissipative solitons in spatially extended systems described by generalized complex Ginzburg-Landau equation on an unbounded domain [27, 55–57]. The case of coupled lasers, however, is distinct in two aspects: (i) unlike the case of complex Ginzburg-Landau equation the presence of the

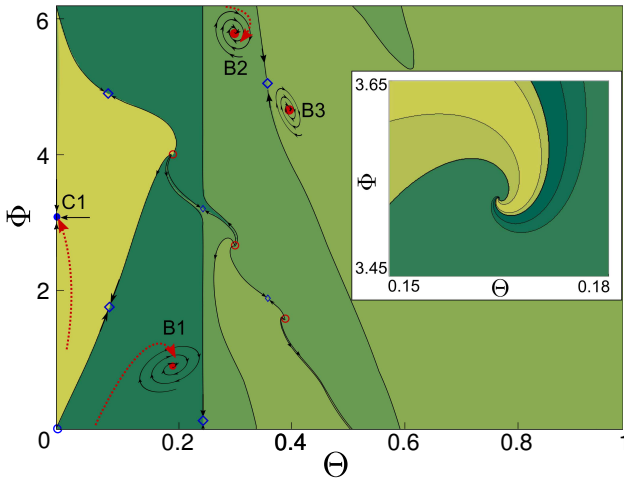


Figure 3. Stable equilibria and their basins of attraction on the phase plane of the reduced system (7) for coupling phase $\varphi = 3.0$. **C1** corresponds to the stable anti-phase synchronized solution. Equilibria **B1**, **B2**, and **B3** correspond to bound states with increasing time separation Θ , which have different phase shifts Φ between pulse intensity maxima. Inset: An example of the intertwining basins of attraction of five stable bound states in the vicinity of a spiral source for the reduced system (7) for $\varphi = 3.99$.

phase shifts $\Delta_{\Theta, \Phi}(\Theta)$ in Eqs. (7) allows for the existence of bound states with the Θ -dependent phase difference between the pulses different from 0 , π , and $\pm\pi/2$, and (ii) instead of a countable set of equidistant roots, the functions $f_{\Theta, \Phi}(\Theta)$ have no roots at all, which means that in laser arrays there is a finite number of bound states which are distributed along the Θ -axis in a more complex manner. The 2D phase plane of the reduced system (7) is presented in Fig. 3, where the equilibria and their basins of attraction are shown. Note, that due to the symmetry $(\Theta, \Phi) \rightarrow (-\Theta, -\Phi)$ it is sufficient to show only the left half of the coordinate system. Here, the point **C1** corresponds to a stable anti-phase synchronized solution, while points **B1**, **B2**, and **B3** indicate the bound states with nonzero pulse time separations Θ . Figure 3 shows the case of $\varphi = 3.0$. For other values of φ , there can co-exist from two to five stable equilibria corresponding to distinct bound states. The basins of attraction of these states are separated by saddles and, interestingly, they can wind into spiral sources as it is shown in the inset of Fig. 3. The video showing the position of the equilibria and corresponding basins of attraction for different values of φ is available in the Supplemental material.

A more detailed stability analysis of the bound state corresponding to the equilibrium **B1** is performed numerically using the path continuation software DDE-BIFTOOL [58] applied to Eqs. (1). The bifurcation diagram showing the domain of stability of this bound state is presented in Fig. 4(b). Here, red line P corresponds to a subcritical pitchfork bifurcation from the in-phase synchronized solution, whereas the blue F line corresponds

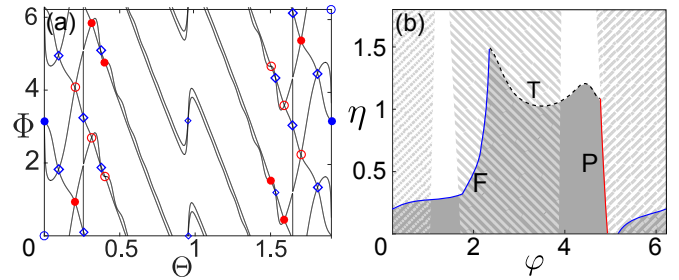


Figure 4. (a) Fixed points and nullclines for the reduced system (7) in the plane (Θ, Φ) calculated for coupling phase $\varphi = 3.0$. Blue filled (empty) circles correspond to stable (unstable) nodes, red filled (empty) circles to stable (unstable) foci, whereas blue empty diamonds to saddles. (b) Bifurcation diagram for the bound state **B1** (cf. Fig. 3, (b)) in the plane (φ, η) . Light gray area shows the stability domain of the bound state. Red line P corresponds to a subcritical pitchfork bifurcation of the in-phase synchronized solution, blue line F corresponds to a fold bifurcation, and dashed black line T indicates the first torus bifurcation. Left- and right-inclined hatching indicates the stability domains of in-phase and anti-phase synchronized solutions from Fig. 1 (a).

to a fold bifurcation leading the appearance of unstable bound state solutions. The dashed black line T shows the first torus bifurcation of pulse bound state which leads to a slight change of the pulse shapes from one pulse period to another, while the period of the pulsing remains the same.

To conclude, we discovered the bound pulse train regime in an array of nearest-neighbor coupled nonlinear distributed dynamical systems. In this regime trains of short pulses generated by individual elements of the array are bound by local interaction, forming the closely packed pulse clusters. In the limit of small coupling strength asymptotic equations are derived governing the slow time evolution positions and phases of the interacting pulses in an array consisting of two pulse generators. The pulse separations and phase differences between the pulses in bound states as well as basins of attraction of different bound states calculated using this semi-analytical approach are in good agreement with the results of direct numerical simulations of a set of DDEs describing an array of coupled mode-locked lasers (1). The stability and bifurcations of bound pulse train regime were studied numerically with the path-following technique. The bound states reported in this Letter have a similarity with rather well studied bound states of dissipative solitons in spatially extended systems, where multiple soliton clusters surrounded by a linearly stable homogeneous regime can be formed due to a similar mechanism of balancing between attraction and repulsion. However, unlike the bound states formed by dissipative solitons, the appearance of this new type of bound states is related to the presence of coupling between the neighboring lasers and it is impossible in a solitary array element, where zero intensity steady state is linearly unstable and

pulse interaction is nonlocal and always repulsive. Furthermore, unlike the case of complex Ginzburg-Landau-type equations, the new bound pulse train regime can exhibit continuously changing phase difference between the pulses depending on their time separation and correspond to a finite number of fixed points distributed non-equidistantly along the time axis. Since the physical mechanism of the bound state formation due to the coupling between neighboring lasers is quite general, it can be observed in other physical systems described by coupled sets of partial or delay differential equations, where pulse solutions are present. Therefore, we believe that

our results are generic and valid for a large class of coupled spatially extended systems of different physical origin.

ACKNOWLEDGMENTS

We thank the German Research Foundation (DFG) for financial support in the framework of the Collaborative Research Center 910, Project A3 and Collaborative Research Center 787, Project B5. A.V. also acknowledges the support of the Grant No. 14-41-00044 of the Russian Scientific Foundation.

-
- [1] N. N. Rosanov, *Spatial Hysteresis and Optical Patterns* (Springer, Berlin, 2002).
- [2] H. Vahed, F. Prati, M. Turconi, S. Barland, and G. Tissoni, *Philosophical Transactions of the Royal Society of London A: Mathematical, Physical and Engineering Sciences* **372** (2014), 10.1098/rsta.2014.0016.
- [3] M. G. Clerc, A. Petrossian, and S. Residori, *Phys. Rev. E* **71**, 015205 (2005).
- [4] F. Arecchi, S. Boccaletti, and P. Ramazza, *Physics Reports* **318**, 1 (1999).
- [5] N. Akhmediev and A. Ankiewicz, eds., *Dissipative Solitons: From Optics to Biology and Medicine*, Lecture Notes in Physics, Vol. 751 (Springer Berlin / Heidelberg, 2008).
- [6] O. Lioubashevski, H. Arbell, and J. Fineberg, *Phys. Rev. Lett.* **76**, 3959 (1996).
- [7] D. J. B. Lloyd, C. Gollwitzer, I. Rehberg, and R. Richter, *Journal of Fluid Mechanics* **783**, 283 (2015).
- [8] H. H. Rotermund, S. Jakubith, A. von Oertzen, and G. Ertl, *Phys. Rev. Lett.* **66**, 3083 (1991).
- [9] A. S. Mikhailov and K. Showalter, *Physics Reports* **425**, 79 (2006).
- [10] H.-G. Purwins, H. U. Bödeker, and S. Amiranashvili, *Adv. in Phys.* **59**, 485 (2010).
- [11] A. W. Liehr, *Dissipative Solitons in Reaction Diffusion Systems. Mechanism, Dynamics, Interaction* (Springer Berlin/Heidelberg, 2013).
- [12] M. Suzuki, T. Ohta, M. Mimura, and H. Sakaguchi, *Phys. Rev. E* **52**, 3645 (1995).
- [13] S. Barland, M. Giudici, G. Tissoni, J. R. Tredicce, M. Brambilla, L. Lugiato, F. Prati, S. Barbay, R. Kuszelewicz, T. Ackemann, W. J. Firth, and G.-L. Oppo, *Nature Photonics* **6**, 204 (2012).
- [14] P. Grelu and N. Akhmediev, *Nature Photonics* **6**, 84 (2012).
- [15] C. Elphick, E. Meron, J. Rinzel, and E. Spiegel, *Journal of Theoretical Biology* **146**, 249 (1990).
- [16] J. N. Kutz, B. C. Collings, K. Bergman, and W. H. Knox, *IEEE Journal of Quantum Electronics* **34**, 1749 (1998).
- [17] M. Nizette, D. Rachinskii, A. Vladimirov, and M. Wolfrum, *Physica D: Nonlinear Phenomena* **218**, 95 (2006).
- [18] P. Camelin, J. Javaloyes, M. Marconi, and M. Giudici, *Phys. Rev. A* **94**, 063854 (2016).
- [19] N. Akhmediev and A. Ankiewicz, *Solitons, Nonlinear Pulses and Beams* (Chapman and Hall, London, 1997).
- [20] N. Akhmediev, A. Ankiewicz, and J. M. Soto-Crespo, *J. Opt. Soc. America B* **15**, 515 (1998).
- [21] P. Grelu, F. Belhache, F. Guty, and J.-M. Soto-Crespo, *Opt. Lett.* **27**, 966 (2002).
- [22] D. Y. Tang, B. Zhao, D. Y. Shen, C. Lu, W. S. Man, and H. Y. Tam, *Phys. Rev. A* **66**, 033806 (2002).
- [23] N. H. Seong and D. Y. Kim, *Opt. Lett.* **27**, 1321 (2002).
- [24] L. M. Zhao, D. Y. Tang, X. Wu, D. J. Lei, and S. C. Wen, *Opt. Lett.* **32**, 3191 (2007).
- [25] C. P. Schenk, P. Schütz, M. Bode, and H.-G. Purwins, *Phys. Rev. E* **57**, 6480 (1998).
- [26] J. H. Lin, C. W. Chan, H. Y. Lee, and Y. H. Chen, *IEEE Photonics Journal* **7**, 1 (2015).
- [27] A. G. Vladimirov, G. V. Khodova, and N. N. Rosanov, *Phys. Rev. E* **63**, 056607 (2001).
- [28] B. Ortaç, A. Zaviyalov, C. K. Nielsen, O. Egorov, R. Iliev, J. Limpert, F. Lederer, and A. Tünnermann, *Opt. Lett.* **35**, 1578 (2010).
- [29] X. Wu, D. Tang, X. Luan, and Q. Zhang, *Optics Communications* **284**, 3615 (2011).
- [30] X. L. Li, S. M. Zhang, Y. C. Meng, Y. P. Hao, H. F. Li, J. Du, and Z. J. Yang, *Laser Physics* **22**, 774 (2012).
- [31] L. Gui, X. Xiao, and C. Yang, *J. Opt. Soc. Am. B* **30**, 158 (2013).
- [32] V. Tsatourian, S. V. Sergeev, C. Mou, A. Rozhin, V. Mikhailov, B. Rabin, P. S. Westbrook, and S. K. Turitsyn, *Scientific Reports* **3**, 3154 EP (2013), article.
- [33] D. Botez and D. R. Scifres, eds., *Diode Laser Arrays*, Cambridge Studies in Modern Optics No. 14 (Cambridge University Press, 2008).
- [34] A. F. Glova, *Quantum Electronics* **33**, 283 (2003).
- [35] H. E. Hagemeyer and S. R. Robinson, *Appl. Opt.* **18**, 270 (1979).
- [36] V. V. Likhanskii and A. P. Napartovich, *Soviet Physics Uspekhi* **33**, 228 (1990).
- [37] R.-d. Li and T. Erneux, *Phys. Rev. A* **46**, 4252 (1992).
- [38] R.-d. Li and T. Erneux, *Phys. Rev. A* **49**, 1301 (1994).
- [39] G. Kozyreff, A. G. Vladimirov, and P. Mandel, *Phys. Rev. Lett.* **85**, 3809 (2000).
- [40] G. Kozyreff, A. G. Vladimirov, and P. Mandel, *Physical Review E* **64**, 016613 (2001).
- [41] A. Jechow, M. Lichtner, R. Menzel, M. Radziunas, D. Skoczowsky, and A. Vladimirov, *Optics Express* **17**, 19599 (2009).

- [42] M. Lichtner, V. Z. Tronciu, and A. G. Vladimirov, *IEEE J. Quant. Electron.* **48**, 353 (2012).
- [43] S. A. Kashchenko, *Computational Mathematics and Mathematical Physics* **38**, 443 (1998).
- [44] G. Giacomelli and A. Politi, *Phys. Rev. Lett.* **76**, 2686 (1996).
- [45] S. Yanchuk, L. Lücken, M. Wolfrum, and A. Mielke, *Discrete Contin. Dyn. Syst. A* **35**, 537 (2015).
- [46] S. Yanchuk and G. Giacomelli, *Journal of Physics A: Mathematical and Theoretical* **50**, 103001 (2017).
- [47] A. G. Vladimirov and D. Turaev, *Phys. Rev. A* **72**, 033808 (2005).
- [48] M. Golubitsky, I. Stewart, and D. G. Schaeffer, *Singularities and Groups in Bifurcation Theory. Volume II*, Applied Mathematical Sciences, Vol. 69 (Springer-Verlag, New-York, 1988) p. 533.
- [49] S. Yanchuk and M. Wolfrum, *Phys. Rev. E* **77**, 026212 (2008).
- [50] O. D’Huys, R. Vicente, T. Erneux, J. Danckaert, and I. Fischer, *Chaos* **18**, 037116 (2008).
- [51] L. M. Pecora and T. L. Carroll, *Physical Review Letters* **80**, 2109 (1998).
- [52] N. Rebrova, G. Huyet, D. Rachinskii, and A. G. Vladimirov, *Phys. Rev. E* **83**, 066202 (2011).
- [53] R. M. Arhipov, T. Habruseva, A. Pimenov, M. Radziunas, S. P. Hegarty, G. Huyet, and A. G. Vladimirov, *J. Opt. Soc. Am. B* **33**, 351 (2016).
- [54] S. Guo and J. Wu, *Bifurcation Theory of Functional Differential Equations*, Applied Mathematical Sciences (Springer New York, 2013).
- [55] D. Turaev, A. G. Vladimirov, and S. Zelik, *Phys. Rev. E* **75**, 045601 (2007).
- [56] B. A. Malomed, *Phys. Rev. A* **44**, 6954 (1991).
- [57] V. V. Afanasjev, B. A. Malomed, and P. L. Chu, *Phys. Rev. E* **56**, 6020 (1997).
- [58] K. Engelborghs, T. Luzyanina, and D. Roose, *ACM Trans. Math. Softw.* **28**, 1 (2002).